JPE 16-5-25

http://dx.doi.org/10.6113/JPE.2016.16.5.1861
ISSN(Print): 1598-2092 / ISSN(Online): 2093-4718

A Three-Phase AC-DC High Step-up Converter for Microscale Wind-power Generation Systems

Lung-Sheng Yang*, Chia-Ching Lin*, and En-Chih Chang†

*Department of Electrical Engineering, Far East University, Tainan, Taiwan
†Department of Electrical Engineering, I-Shou University, Kaohsiung, Taiwan

Abstract

In this paper, a three-phase AC-DC high step-up converter is developed for application to microscale wind-power generation systems. Such an AC-DC boost converter prossessess the property of the single-switch high step-up DC-DC structure. For power factor correction, the advanced half-stage converter is operated under the discontinuous conduction mode (DCM). Simulatanously, to achieve a high step-up voltage gain, the back half-stage functions in the continuous conduction mode (CCM). A high voltage gain can be obtained by use of an output-capacitor mass and a coupled inductor. Compared to the output voltage, the voltage stress is decreased on the switch. To lessen the conducting losses, a low rated voltage and small conductive resistance MOSFETs are adopted. In addition, the coupled inductor retrieves the leakage-inductor energy. The operation principle and steady-state behavior are analyzed, and a prototype hardware circuit is realized to verify the performance of the proposed converter.

Key words: Boost converter, High step-up converter, Power factor correction

I. INTRODUCTION

Since the world population is rapidly growing, the demand for energy is rising and fossil fuels, including oil, gas, and coal are gradually being depleted. In addition, utilizing fossil fuels has resulted in a rapid accumulation of carbon dioxide in the past few decades. This has resulted in greenhouse effects and abnormal global climate changes. In an effort to solve this energy shortage and to reduce pollution, sustainable power sources, namely photovoltaic, wind-power, geothermal, hydraulic, hydro, biomass, etc., are being gradually developed [1]-[5]. In wind energy generating systems, the output-voltage and frequency of the generator are varied due to wind speed. Thus, their ranges are very large. Traditionally, a bridge-diode rectifier in combination with a DC-DC structure is adopted in converting AC to DC power for wind energy generating systems, as shown in Fig. 1(a) [6]-[8]. This results in a large pulsating input current and large current stresses in the generator windings. To resolve these difficulties, various circuits have been presented for power factor correction, including buck type [9]-[11], boost type [12]-[14], and buck-boost type [15]-[18]. These converters can be operated in the continuous conduction mode (CCM) or the discontinuous conduction mode (DCM). As a result, a higher power factor and lower current stresses for the generator can be achieved. For wind-power generation systems, grid-connection is the main application. For the purpose of boosting the output-voltage in a generator, a high DC voltage must be produced, as shown in Fig. 1(b). Although Boost converters can be applied for the conversion of step-up voltage, a high voltage gain cannot be provided, which has led to the study of high gain step-up converters [19]-[24].

A single-stage three-phase AC-DC converter with a high step-up structure was investigated for micro-scale wind-power generation systems, as shown in Fig. 2(a). Some of the part contents have been presented in the literature [25]. This type of converter utilizes a single switch to integrate a conventional three-phase AC-DC boost converter and a high step-up DC-DC structure with a coupled inductor [26]-[30]. The presented converter yields a high power factor, which alleviates the large pulsating current and reducing the current stresses of the generator windings. For the sake of power factor correction, the advanced half-stage circuitry, i.e., a

Manuscript received Aug. 5, 2015; accepted Dec. 14, 2015
Recommended for publication by Associate Editor Dong-Myung Lee.
†Corresponding Author: enchihchang@isu.edu.tw
Tel: +886-7-6577711-6642, I-Shou University
*Department of Electrical Engineering, Far East University, Taiwan

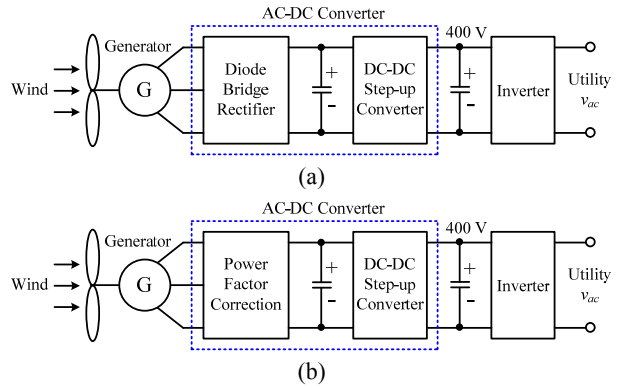

Fig. 1. Wind-power generation system. (a) Diode-bridge rectifier type, (b) Power factor correction type.

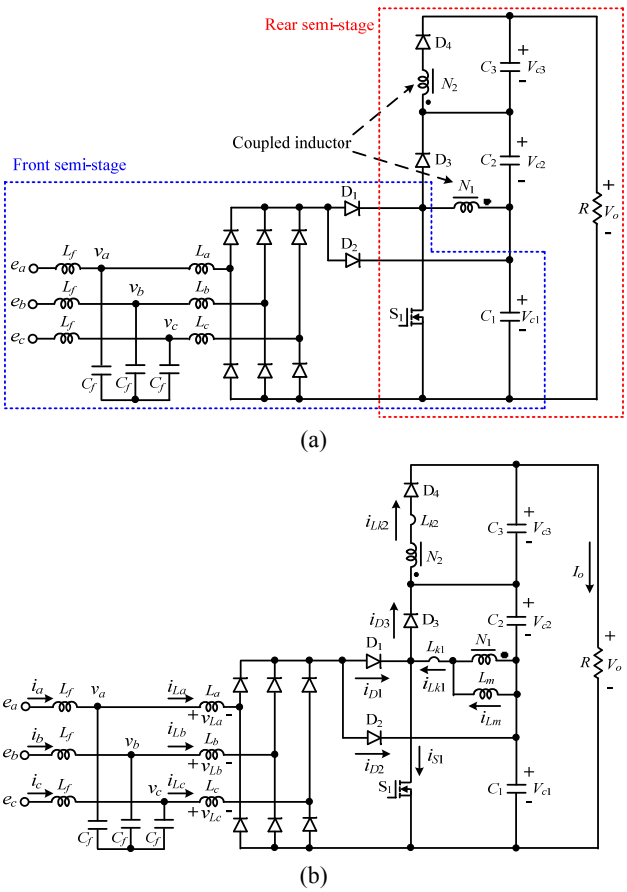

Fig. 2. Proposed converter. (a) Circuit configuration, (b) Simplified circuit model.

three-phase AC-DC boost converter is fulfilled in the DCM while the back half-stage associated with the output-capacitor stack and coupled-inductor techniques works in the CCM for a high gain step-up voltage. In addition, the active-clamp function is achieved and smaller switch voltage stress yields are obtained when compared with the output-voltage. It is worth mentioning that the decreased losses in conducting can be obtained by low rated voltage and small conductive resistance MOSFETs. In addition, the leakage-inductor energy of the coupled inductor is also regained.

II. Operating Principles

Fig. 2(b) reveals a simplified circuitry model of the proposed converter. The coupled inductor can be represented by a magnetizing inductor L_m, a primary leakage inductor L_{k1}, a secondary leakage inductor L_{k2}, and an ideal transformer. To analyze the circuitry simply, the following circumstances are supposed: 1) Allow all of the elements to be ideal. That is, omit the ON-state resistance $R_{ds(on)}$ of the active switch, the forward voltage drop of the diodes, and the equivalent series resistance of the coupled inductor and output capacitors. 2) When the output capacitors C_1, C_2, and C_3 are sufficiently large, the voltages across these capacitors can be regarded as constant at the each switching duration.

The pulse-width-modulation technology is applied for controlling the switch S_1. The advanced half-stage of the proposed converter is performed under the DCM. The back half-stage of the proposed converter is fulfilled under the CCM. The inductances of the three input inductors are equal, namely $L_a = L_b = L_c = L$. Because a three-phase system is symmetrical, the principle of operation is explored within [0°, 30°]. Several classic waveforms at a duration of one switching can be illustrated as in Fig. 3.

(1) Mode 1, [hT_s, t_{h1}]: Fig. 4(a) shows the direction of the current-flow. When the switch S_1 is turned on, the energies of the three input inductors L_a, L_b, and L_c are reserved through line source. The absolute values of the currents i_{La}, i_{Lb}, and i_{Lc} raise, and the sum of the absolute values of the currents i_{La} and i_{Lc} agree with the absolute value of the current i_{Lb}. The capacitor C_1 delivers energy to the magnetizing inductor L_m and primary leakage inductor L_{k1} owned by coupled inductor. The secondary leakage inductor L_{k2} owned by the coupled inductor retrieves energy to the capacitor C_3. Therefore, the magnetizing-inductor current i_{Lm} and primary leakage-inductor current i_{Lk1} are raised and the secondary leakage-inductor current i_{Lk2} is reduced. The stacked energies from the capacitors C_1, C_2, and C_3 can provide the load. At $t = t_{k1}$, the energy storage by the secondary leakage inductor L_{k2} is empty. The current i_{Lk1} is equal to the current i_{Lm}.

(2) Mode 2, [t_{h1}, t_{h2}]: Fig. 4(b) shows the direction of the current-flow, and the switch S_1 turns on. The energies of the three input inductors L_a, L_b, and L_c are continuously derived via the line source. Therefore, the absolute values of the currents i_{La}, i_{Lb}, and i_{Lc}, still raise, and the sum of the absolute values of the currents i_{La} and i_{Lc} agrees with the absolute value of the current i_{Lb}. The capacitor C_1 still delivers energy to the magnetizing inductor L_m and primary leakage inductor L_{k1}. The currents i_{Lm} and i_{Lk1} are increased, and the stacked energies from the capacitors C_1, C_2, and C_3 are provided to the load.

(3) Mode 3, [t_{h2}, t_{h3}]: Fig. 4(c) indicates the direction of the current-flow, and the switch S_1 turns off. The three input inductors L_a, L_b, and L_c deliver energies to C_1. Therefore, the absolute values of the currents i_{La}, i_{Lb}, and i_{Lc} are reduced, and the sum of the absolute values of the currents i_{La} and i_{Lc}

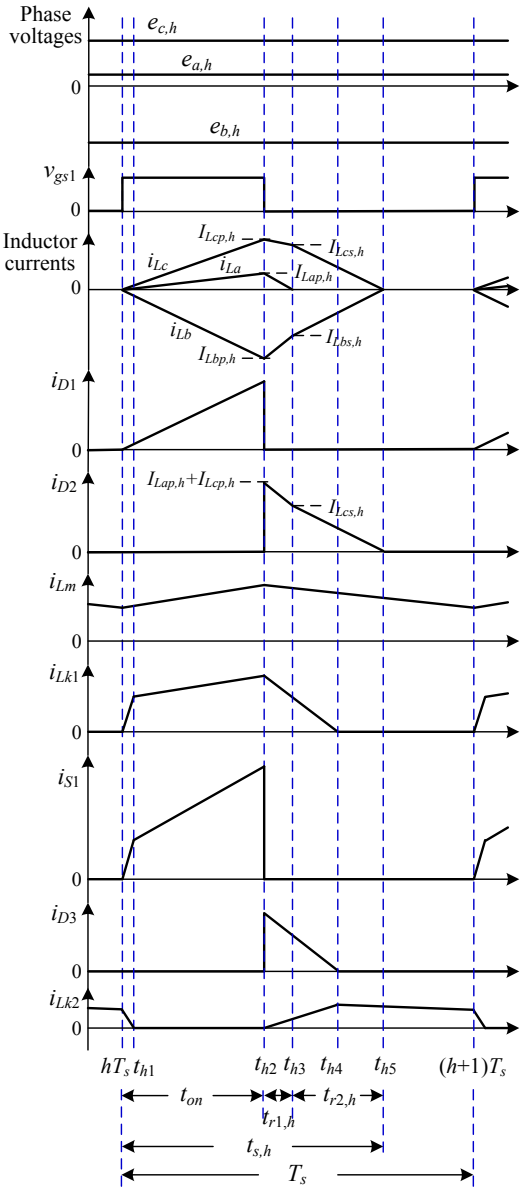

Fig. 3. Some waveforms in one switching period during [0°, 30°].

agrees with the absolute value of the current i_{Lb}. The magnetizing inductor L_m and primary leakage inductor L_{k1} owned by the coupled inductor deliver energies to the capacitor C_2, and the magnetizing inductor L_m discharges part of the energy to the secondary leakage inductor L_{k2} and capacitor C_3. Therefore, the currents i_{Lm} and i_{Lk1} are decreased and the current i_{Lk2} is increased. The primary leakage inductor L_{k1} retrieves the energy from the capacitor C_2. The stacked energies from the capacitors C_1, C_2, and C_3 are provided to the load. At $t = t_{k3}$, there is a blank energy storage by the inductor L_a.

(4) Mode 4, [t_{h3}, t_{h4}]: Fig. 4(d) reveals the direction of the current-flow, and the switch S_1 turns off. The inductors L_b and L_c continuously deliver energies to the capacitor C_1. Therefore, the absolute values of the currents i_{Lb} and i_{Lc}

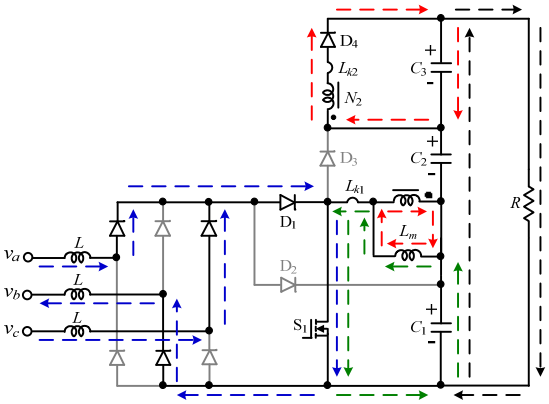

(a) Mode 1.

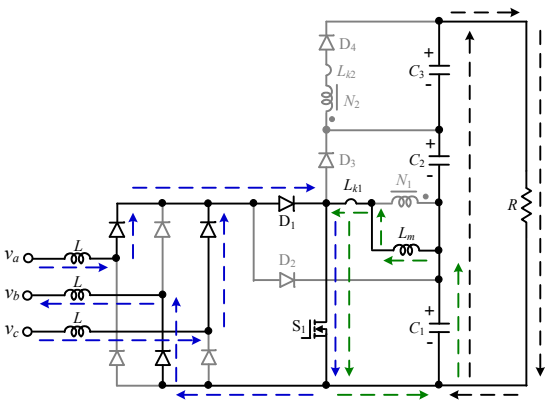

(b) Mode 2.

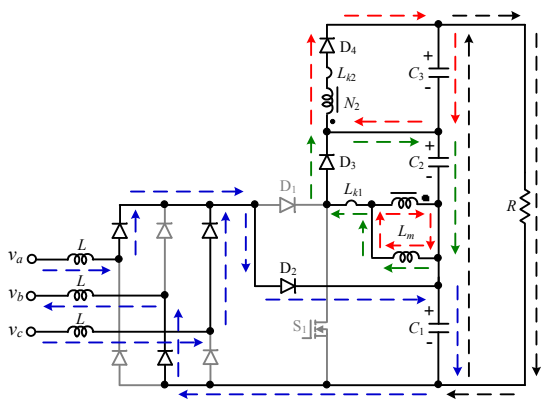

(c) Mode 3.

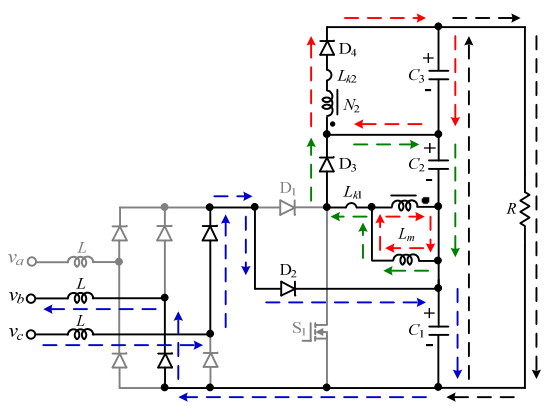

(d) Mode 4.

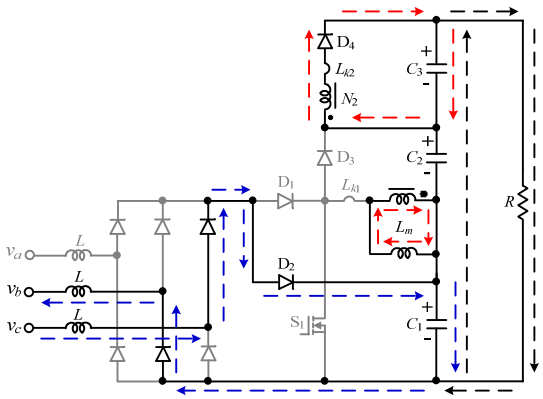

(e) Mode 5.

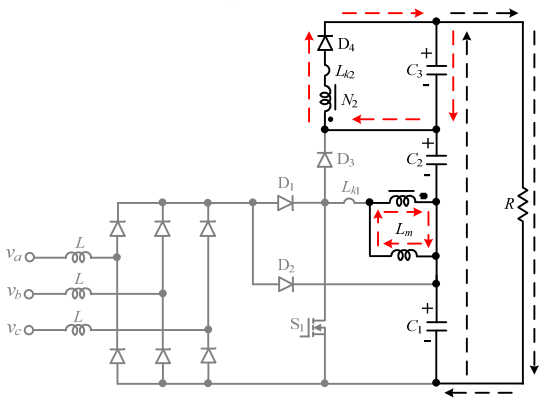

(f) Mode 6.

Fig. 4. Current-flow path of proposed converter during [0°, 30°].

reduce, and the absolute value of the current i_{Lb} agrees with the absolute value of the current i_{Lc}. The magnetizing inductor L_m and the primary leakage inductor L_{k1} deliver energies to the capacitor C_2, and the magnetizing inductor L_m discharges part of the energy to the secondary leakage inductor L_{k2} and the capacitor C_3. Therefore, the currents i_{Lm} and i_{Lk1} are decreased, and the current i_{Lk2} is increased. Meanwhile, the primary leakage inductor L_{k1} retrieves energy from the capacitor C_2. The stacked energies from the capacitors C_1, C_2, and C_3 are provided to the load. At $t = t_{h4}$, the energy storage by the primary leakage inductor L_{k1} is empty.

(5) Mode 5, [t_{h4}, t_{h5}]: Fig. 4(e) shows the direction of the current-flow, and the switch S_1 turns off. The inductors L_b and L_c deliver energies to the capacitor C_1. Therefore, the absolute values of the currents i_{Lb} and i_{Lc} are reduced and the absolute value of the current i_{Lb} agrees with the absolute value of the current i_{Lc}. The magnetizing inductor L_m and secondary leakage inductor L_{k2} discharge energies to the capacitor C_3. Therefore, the currents i_{Lm} and i_{Lk2} are decreased. Meanwhile, the secondary leakage inductor L_{k2} retrieves the energy from the capacitor C_3. The stacked energies from the capacitors C_1, C_2, and C_3 are provided to the load. At $t = t_{h5}$, there are blank energy storages by the inductors L_b and L_c.

(6) Mode 6, [t_{h5}, $(h+1)T_s$]: Fig. 4(f) denotes the direction of the current-flow, and the switch S_1 turns off. The magnetizing inductor L_m and secondary leakage inductor L_{k2} discharge energies to the capacitor C_3. Thus, the currents i_{Lm} and i_{Lk2} are decreased. Meanwhile, the secondary leakage inductor L_{k2} retrieves the energy from the capacitor C_3. The stacked energies from the capacitors C_1, C_2, and C_3 are provided to the load.

III. Steady-State Analysis

A. Front Semi-Stage of the Proposed Converter

Because the three-phase system provides a symmetrization property, the steady-state behavior is analyzed below for the duration of [0°, 30°]. Briefly, omit the influence caused by the input filter and assume that the three input phase voltages are:

$$\begin{cases} e_a(t) = v_a(t) = V_m \sin \omega t \\ e_b(t) = v_b(t) = V_m \sin(\omega t - 120^\circ) \\ e_c(t) = v_c(t) = V_m \sin(\omega t - 240^\circ) \end{cases} \tag{1}$$

where V_m denotes the amplitude of the input phase voltage.

Since the switching frequency f_s is far bigger than the line frequency f_1, the input phase voltages can be regarded as a piecewise constant for the duration of each switching period. Let the parameter m be the switching number at the duration of [0°, 30°]. Then the parameter m is equal to $f_s/12f_1$. The analysis in the following is investigated within the switching period $[hT_s, (h+1)T_s]$, where h = 0, 1,..., m-1. While the switch S_1 is turned on, the equations yields:

$$\begin{cases} \dfrac{di_{La}(t)}{dt} = \dfrac{e_a(hT_s)}{L} \\ \dfrac{di_{Lb}(t)}{dt} = \dfrac{e_b(hT_s)}{L}, \\ \dfrac{di_{Lc}(t)}{dt} = \dfrac{e_c(hT_s)}{L} \end{cases} \qquad kT_s \le t \le t_{h2} \tag{2}$$

Thus, the currents i_{La}, i_{Lb}, and i_{Lc} are obtained as follows:

$$\begin{cases} i_{La}(t) = \dfrac{e_a(hT_s)}{L}(t - hT_s) \\ i_{Lb}(t) = \dfrac{e_b(hT_s)}{L}(t - hT_s), \\ i_{Lc}(t) = \dfrac{e_c(hT_s)}{L}(t - hT_s) \end{cases} \qquad hT_s \le t \le t_{h2} \tag{3}$$

At $t = t_{h2}$, the peak values of i_{La}, i_{Lb}, and i_{Lc} are found to be:

$$\begin{cases} I_{Lap,h} = \dfrac{e_a(hT_s)}{L} t_{on} = \dfrac{e_a(hT_s)}{L} DT_s \\ I_{Lbp,h} = \dfrac{e_b(hT_s)}{L} t_{on} = \dfrac{e_b(hT_s)}{L} DT_s \\ I_{Lcp,h} = \dfrac{e_c(hT_s)}{L} t_{on} = \dfrac{e_c(hT_s)}{L} DT_s \end{cases} \tag{4}$$

where D indicates the duty ratio.

Within $[t_{h2}, (h+1)T_s]$, the switch S_1 turns off. During $[t_{h2}, t_{h3}]$, the formulas can be obtained by Fig. 4(c).

$$\begin{cases} e_a(kT_s) = v_{La}(t) + V_{c1} - v_{Lb}(t) + e_b(kT_s) \\ e_a(kT_s) = v_{La}(t) - v_{Lc}(t) + e_c(kT_s) \\ v_{La}(t) + v_{Lb}(t) + v_{Lc}(t) = 0 \end{cases}, \quad t_{k2} \le t \le t_{k3} \tag{5}$$

Through the use of (5), the voltages across the inductors L_a, L_b, and L_c are derived as:

$$\begin{cases} v_{La}(t) = e_a(hT_s) - \dfrac{V_{c1}}{3} \\ v_{Lb}(t) = e_b(hT_s) + \dfrac{2V_{c1}}{3}, \quad t_{h2} \le t \le t_{h3} \\ v_{Lc}(t) = e_c(hT_s) - \dfrac{V_{c1}}{3} \end{cases} \tag{6}$$

From Fig. 3, the voltages v_{La}, v_{Lb}, and v_{Lc} can also be determined as follows:

$$\begin{cases} v_{La}(t) = L\dfrac{di_{La}}{dt} = \dfrac{-LI_{Lap,h}}{t_{r1,h}} \\ v_{Lb}(t) = L\dfrac{di_{Lb}}{dt} = \dfrac{L(I_{Lbs,h} - I_{Lbp,h})}{t_{r1,h}}, \quad t_{h2} \le t \le t_{h3} \\ v_{Lc}(t) = L\dfrac{di_{Lc}}{dt} = \dfrac{L(I_{Lcs,h} - I_{Lcp,h})}{t_{r1,h}} \end{cases} \tag{7}$$

where $t_{r1,h} = t_{h3} - t_{h2}$.

Substituting (4) and (6) into (7), the interval $t_{r1,h}$ is obtained as:

$$t_{r1,h} = \frac{3DT_s e_a(hT_s)}{V_{c1} - 3e_a(hT_s)} \tag{8}$$

(7) can be replaced by (4), (6) and (8), and then it is possible to obtain:

$$\begin{cases} I_{Lbs,h} = \dfrac{DT_s V_{c1}\left[2e_a(hT_s) + e_b(hT_s)\right]}{L\left[V_{c1} - 3e_a(hT_s)\right]} \\ I_{Lcs,h} = \dfrac{DT_s V_{c1}\left[-e_a(hT_s) + e_c(hT_s)\right]}{L\left[V_{c1} - 3e_a(hT_s)\right]} \end{cases} \tag{9}$$

During $[t_{h3}, t_{h5}]$, it is possible to obtain the formulas below by means of Figs. 4(d) and 4(e).

$$\begin{cases} e_b(hT_s) = v_{Lb}(t) - V_{c1} - v_{Lc}(t) + e_c(hT_s) \\ v_{Lb}(t) + v_{Lc}(t) = 0 \end{cases}, \quad t_{h3} \le t \le t_{h5} \tag{10}$$

Thus:

$$\begin{aligned} v_{Lb}(t) = -v_{Lc}(t) &= \frac{e_b(hT_s) - e_c(hT_s) + V_{c1}}{2} \\ &= L\frac{di_{Lb}(t)}{dt} = \frac{-LI_{Lbs,h}}{t_{r2,h}}, \quad t_{h3} \le t \le t_{h5} \end{aligned} \tag{11}$$

where $t_{r2,h} = t_{h5} - t_{h3}$.

Substituting (9) into (11), yields:

$$t_{r2,h} = \frac{-2DT_s V_{c1}\left[2e_a(hT_s) + e_b(hT_s)\right]}{\left[V_{c1} + e_a(hT_s) + 2e_b(hT_s)\right]\left[V_{c1} - 3e_a(hT_s)\right]} \tag{12}$$

B. Rear Semi-Stage of the Proposed Converter

While the switch S_1 turns, the voltage across the magnetizing inductor L_m can be derived as:

$$v_{Lm(\text{on})} = \frac{L_m}{L_m + L_{k1}} V_{c1} = kV_{c1} \tag{13}$$

where the coupling coefficient k of the coupled-inductor agrees with $L_m/(L_m+L_{k1})$. Therefore:

$$i_{Lm(\text{on})} = \frac{kV_{c1}}{L_m}(t - hT_s), \quad hT_s \le t \le t_{h2} \tag{14}$$

While the switch S_1 turns off, the following equation is obtained:

$$v_{Lm(\text{off})} = -\frac{v_{Lk2} + V_{c3}}{n} \tag{15}$$

where the turns ratio n of the coupled inductor agrees with N_2/N_1. Owing to $k = L_m/(L_m+L_{k1})$:

$$L_{k1} = \frac{(1-k)L_m}{k} \tag{16}$$

$$L_{k2} = \frac{n^2(1-k)L_m}{k} \tag{17}$$

Thus:

$$v_{Lk2} = L_{k2}\frac{di_{Lk2}}{dt} = n^2 L_{k1}\frac{di_{Lk2}}{dt} = nL_{k1}\frac{di_{Lm}}{dt} \tag{18}$$

Substituting (16) into (18), yields:

$$v_{Lk2} = \frac{n(1-k)L_m}{k} \times \frac{di_{Lm}}{dt} = \frac{n(1-k)}{k} v_{Lm(\text{off})} \tag{19}$$

Substituting (19) into (15), yields:

$$v_{Lm(\text{off})} = -\frac{kV_{c3}}{n} \tag{20}$$

Therefore:

$$i_{Lm(\text{off})} = -\frac{kV_{c3}}{nL_m}(t - t_{h2}), \quad t_{h2} \le t \le (h+1)T_s \tag{21}$$

By the principle of the volt-second balance acted on by the magnetizing inductor L_m, it is possible to obtain:

$$v_{Lm(\text{on})}DT_s + v_{Lm(\text{off})}(1-D)T_s = 0 \tag{22}$$

(21) is replaced by (13) and (19). Then the equations become:

$$V_{c3} = \frac{nD}{1-D} V_{c1} \tag{23}$$

From the operating principle, it is known that L_{k1} retrieves energy from the capacitor C_1. By the principle of the ampere-second balance on C_1, the voltage across C_1 can be obtained as follows [31]:

$$V_{c2} = \frac{D[(1+k) + n(1-k)]}{2(1-D)} V_{c1} \tag{24}$$

Then:

$$V_o = \left\{\frac{1 + (n-1)D}{1-D} + \frac{D[(1+k) + n(1-k)]}{2(1-D)}\right\} V_{c1} \tag{25}$$

At $k = 1$, equation (25) can be rewritten as:

$$V_o = \frac{1+nD}{1-D} V_{c1} \tag{26}$$

Therefore, the proposed converter can provide a high voltage gain.

IV. Experimental Results

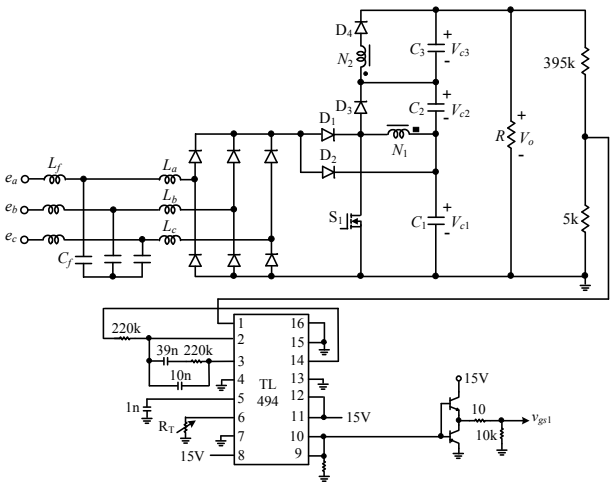

Fig. 5. Proposed converter with control circuit.

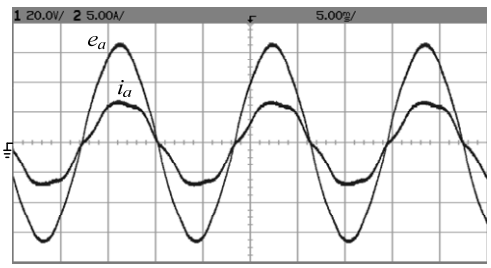

e_a: 20 V/div, i_a: 5 A/div, Time: 5 ms/div

(a)

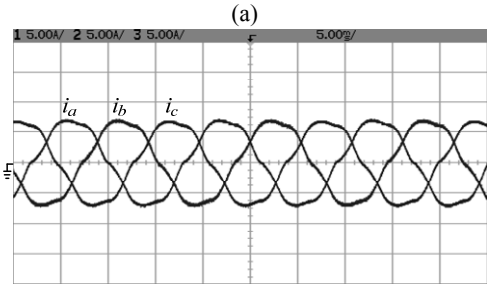

$i_a/i_b/i_c$: 5 A/div, Time: 5 ms/div

(b)

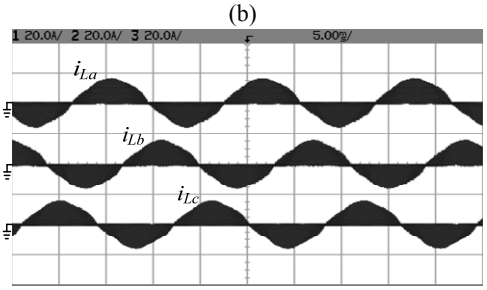

$i_{La}/i_{Lb}/i_{Lc}$: 20 A/div, Time: 5 ms/div

(c)

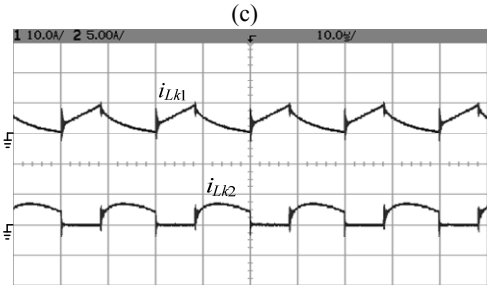

i_{Lk1}: 10 A/div, i_{Lk2}: 5 A/div,Time: 10 μs/div

(d)

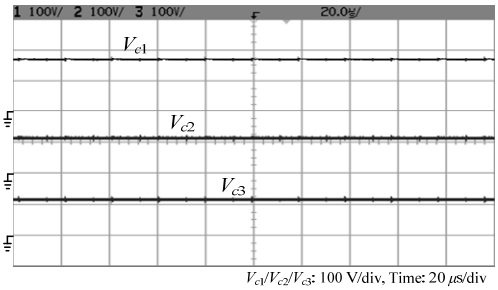

$V_{c1}/V_{c2}/V_{c3}$: 100 V/div, Time: 20 μs/div

(e)

Fig. 6. Some experimental waveforms at full-load conditions V_{in}/f_1 = 80 V_{rms}/62 Hz, V_o = 400 V, and P_o = 600 W. (a) Input phase voltage and input phase current. (b) Three input phase currents. (c) Three input inductor currents. (d) Leakage-inductor currents i_{Lk1} and i_{Lk2}. (e) Three output-capacitor voltages.

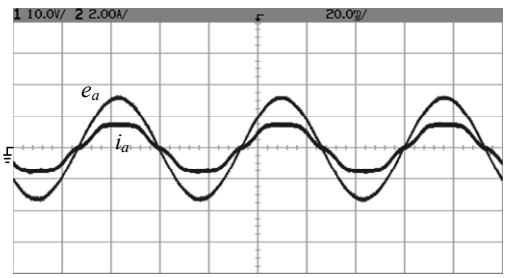

e_a: 10 V/div, i_a: 2 A/div, Time: 20 ms/div

(a)

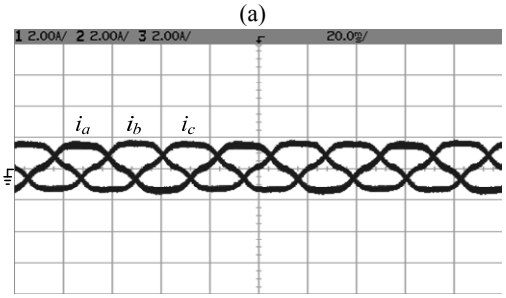

$i_a/i_b/i_c$: 2 A/div, Time: 20 ms/div

(b)

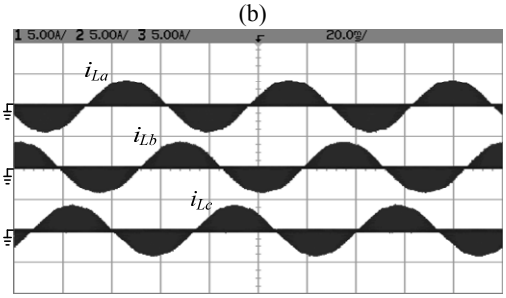

$i_{La}/i_{Lb}/i_{Lc}$: 5 A/div, Time: 20 ms/div

(c)

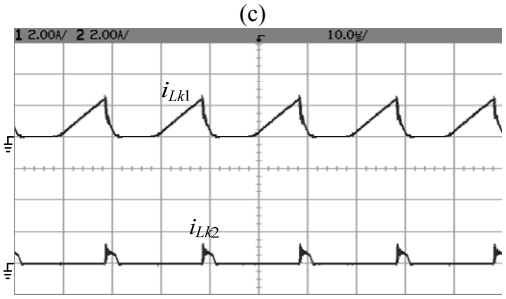

i_{Lk1}/i_{Lk2}: 2 A/div,Time: 10 μs/div

(d)

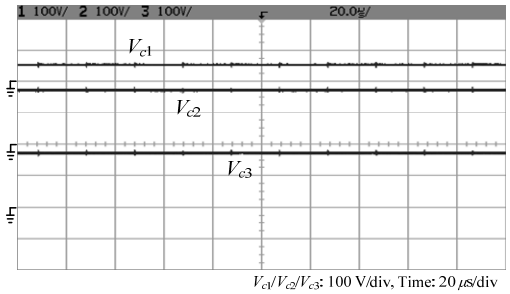

(e)

Fig. 7. Some experimental waveforms at light-load conditions V_{in}/f_1 = 20 V_{rms}/15 Hz, V_o = 400 V, and P_o = 30 W. (a) Input phase voltage and input phase current. (b) Three input phase currents. (c) Three input inductor currents. (d) Leakage-inductor currents i_{Lk1} and i_{Lk2}. (e) Three output-capacitor voltages.

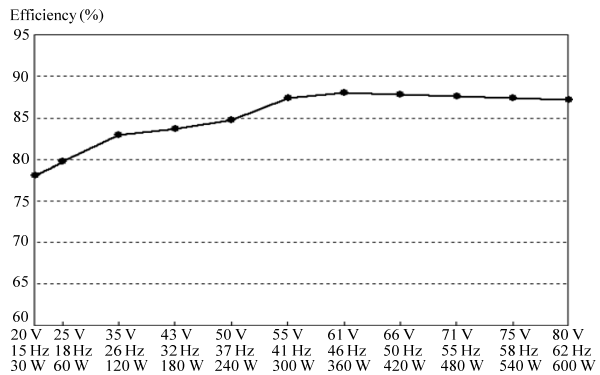

Fig. 8. Measured efficiency at V_{in}/f_1 = 20 V_{rms}/15 Hz~80 V_{rms}/62 Hz, V_o = 400 V, and P_o = 30~600 W.

A laboratory prototype is realized to demonstrate the effectiveness of the proposed converter for micro-scale wind-power generation systems. The output voltage and frequency produced by the three-phase generator match the input voltage and frequency created by the proposed converter. The system parameters of the proposed converter are chosen as: input voltage/frequency V_{in}/f_1 = 20V_{rms}/15Hz ~ 80V_{rms}/62Hz, output voltage V_o = 400 V, output power P_o = 600 W, switching frequency f_s = 50 kHz, input inductor L = 34 μH, coupled inductor L_m = 205 μH (turns ratio n = 1), capacitors C_1 = 820 μF, C_2 = C_3 = 220 μF, input filter L_f = 2.4 mH, C_f = 2 μF, switch S_1: IXFK64N50P, and diodes D_1~D_4: DSEP30-06A.

Fig. 5 shows a circuit diagram of the proposed converter with its control circuitry. Figs. 6 and 7 show some experimental waveforms under full-load conditions, V_{in}/f_1 = 80 V_{rms}/62 Hz and P_o = 600 W, and light-load conditions, V_{in}/f_1 = 20 V_{rms}/15 Hz and P_o = 30 W. It can be seen from Figs. 6(a) and 7(a) that the input phase voltage and input phase current are in phase. Figs. 6(b) and 7(b) show the waveforms of the three input currents. It can be seen that the current stress is reduced for the generator winding. The waveforms of the input inductor currents i_{La}, i_{Lb}, and i_{Lc} are represented in Figs. 6(c) and 7(c). It can be seen that the advanced half-stage is performed under the DCM. Figs. 6(d) and 7(d) show the waveforms of the leakage-inductor currents i_{Lk1} and i_{Lk2}. Waveforms of the three output-capacitor voltages are plotted in Figs. 6(e) and 7(e). It can be seen that the sum of V_{c1}, V_{c2}, and V_{c3} agrees with the output voltage. Fig. 8 shows the efficiency of the measurements under various conditions. The maximal efficiency is 88% at V_{in}/f_1 = 61 V_{rms}/46 Hz, V_o = 400 V, and P_o = 360 W.

V. Conclusions

A three-phase high step-up AC-DC converter is researched for micro-scale wind power generation systems. The advanced half-stage of the proposed converter can provide a high power factor. Output-capacitor stack and coupled inductor technologies are used for the back half-stage of the proposed converter to achieve a high voltage gain. Additionally, the energy of the leakage-inductor can be retrieved. A laboratory prototype is realized to confirm the theoretical analysis. From the experimental results, it can be seen that a high power factor and a high voltage gain can be obtained for different input line voltages/frequencies and output powers.

References

[1] B. Kroposki, P. K. Sen, and K. Malmedal, "Selection of distribution feeders for implementing distributed generation and renewable energy applications," *IEEE Trans. Ind. Appl.*, Vol. 49, No. 6, pp. 2825-2834, Nov./Dec. 2013.

[2] W. Chen, X. Wu, L. Yao, W. Jiang, and R. Hu, "A step-up resonant converter for grid-connected renewable energy sources," *IEEE Trans. Power Electron.*, Vol. 30, No. 6, pp. 3017-3029, Jun. 2015.

[3] S. K. Kwon and K. F. A. Sayed, "Boost-half bridge single power stage PWM DC-DC converters for PEM-fuel cell stacks," *Journal of Power Electronics*, Vol. 8, No. 3, pp. 239-247, May 2008.

[4] Y. Yang, K. T. Mok, S. C. Tan, and S. Y. Hui, "Nonlinear dynamic power tracking of low-power wind energy conversion system," *IEEE Trans. Power Electron.,* Vol. 30, No. 9, pp. 5223-5236, Sep. 2015.

[5] J. M. Kwon, B. H. Kwon, and K. H. Nam, "High-efficiency module-integrated photovoltaic power conditioning system," *IET Power Electron*ics, Vol. 2, No. 4, pp. 410-420, Jul. 2009.

[6] K. Y. Lo, Y. M. Chen, and Y. R. Chang, "MPPT battery charger for stand-alone wind power system," *IEEE Trans. Power Electron.,* Vol. 26, No. 6, pp. 1631-1638, Jun. 2011.

[7] T. Ahmedy, K. Nishida, and M. Nakaoka, "Wind power grid integration of an IPMSG using a diode rectifier and a simple MPPT control for grid-side inverters," *Journal of Power Electronics*, Vol. 10, No. 5, pp. 548-554, Sep. 2010.

[8] J. Chen, J. Chen, and C. Gong, "New overall power control strategy for variable-speed fixed-pitch wind turbines within the whole wind velocity range," *IEEE Trans. Ind. Electron.*, Vol. 60, No. 7, pp. 2652-2660, Jul. 2013.

[9] A. Trentin, P. Zanchetta, P. Wheeler, and J. Clare, "Performance evaluation of high-voltage 1.2 kV silicon carbide metal oxide semi-conductor field effect transistors

for three-phase buck-type PWM rectifiers in aircraft applications," *IET Power Electronics*, Vol. 5, No. 9, pp. 1873-1881, Nov. 2012.
[10] A. A. Badin and I. Barbi, "Unity power factor isolated three-phase rectifier with two single-phase buck rectifiers based on the scott transformer," *IEEE Trans. Power Electron.,* Vol. 26, No. 9, pp. 2688-2696, Sep. 2011.
[11] S. K. Bassan, D. S. Wijeratne, and G. Moschopoulos, "A three-phase reduced-switch high-power-factor buck-type converter," *IEEE Trans. Power Electron.,* Vol. 25, No. 11, pp. 2772-2785, Nov. 2010.
[12] B. Singh and P. Venkateswarlu, "A simplified control algorithm for three-phase, four-wire unified power quality conditioner," *Journal of Power Electronics*, Vol. 10, No. 1, pp. 91-96, Jan. 2010.
[13] S. W. Choi and Y. S. Bae, "A new unity power factor rectifier system using an active waveshaping technique," *Journal of Power Electronics*, Vol. 9, No. 2, pp. 173-179, Mar. 2009.
[14] C. T. Pan and Y. L. Juan, "A novel sensorless MPPT controller for a high-efficiency microscale wind power generation system," *IEEE Trans. Energy Convers.*, Vol. 25, No. 1, pp. 207-216, Mar. 2010.
[15] L. S. Yang, T. J. Liang, and J. F. Chen, "Analysis and design of a novel three-phase AC-DC buck-boost converter," *IEEE Trans. Power Electron.,* Vol. 23, No. 2, pp. 707-714, Mar. 2008.
[16] D. S. Wijeratne and G. Moschopoulos, "A novel three-phase buck-boost AC-DC converter," *IEEE Trans. Power Electron.,* Vol. 29, No. 3, pp. 1331-1343, Mar. 2014.
[17] L. S. Yang, T. J. Liang, J. F. Chen, and R. L. Lin, "Analysis and design of a novel single-stage three-phase AC/DC step-down converter with electrical isolation," *IET Power Electronics*, Vol. 1, No. 1, pp. 154-163, Mar. 2008.
[18] L. S. Yang, T. J. Liang, and J. F. Chen, "Analysis and design of a single-phase buck-boost power-factor-correction circuit for universal input voltage," in 33rd Annual Conference of the *IEEE Industrial Electronics Society (IECON)*, pp. 1461-1465, Nov. 2007.
[19] M. Prudente, L. L. Pfitscher, G. Emmendoerfer, E. F. Romaneli, and R. Gules, "Voltage multiplier cells applied to non-isolated DC-DC converters," *IEEE Trans. Power Electron.*, Vol. 23, No. 2, pp. 871-887, Mar. 2008.
[20] L. S. Yang, T. J. Liang, H. C. Lee, and J. F. Chen, "Novel high step-up DC-DC converter with coupled-inductor and voltage-doubler circuits," *IEEE Trans. Ind. Electron.*, Vol. 58, No. 9, pp. 4196-4206, Sep. 2011.
[21] P. Das and G. Moschopoulos, "An integrated dc-dc power converter for use in distributed generation power systems," in *IEEE International Telecommunications Energy Conference*, 2008.
[22] C. M. Wang, J. H. Su, and C. H. Yang, "A novel ZCS-PWM flyback converter with a simple ZCS-PWM auxiliary circuit," in *IEEE International Conference on Power Electronics and Drives Systems*, Vol. 1, pp. 805-810, 2005.
[23] Y. P. Hsieh, J. F. Chen, T. J. Liang, and L. S. Yang, "Novel high step-up DC-DC converter with coupled-inductor and switched-capacitor techniques," *IEEE Trans. Ind. Electron.*, Vol. 59, No. 2, pp. 998-1007, Feb. 2012.
[24] S. Y. Tseng, J. Z. Shiang, W. S. Jwo, and C. M. Yang, "Active clamp interleaved boost converter with coupled inductor for high step-up ratio application," in *IEEE 7th International Conference on Power Electronics and Drive Systems*, pp. 1394-1400, Nov. 2007.
[25] L. S. Yang, M. S. Li, T. J. Liang, and J. F. Chen, "Study and implementation of a single-stage three-phase AC-DC converter," in *IEEE 6th International Power Electronics and Motion Control Conference (IPEMC)*, pp.683-688, May 2009.
[26] K. Yao, X. Ruan, C. Zou, and Z. Ye, "Three-phase single-switch boost power factor correction converter with high input power factor," *IET Power Electronics*, Vol. 5, No. 7, pp. 1095-1103, Aug. 2012.
[27] D. S. L. Simonetti, J. L. F. Vieira, and G. C. D. Sousa, "Modeling of the high-power-factor discontinuous boost rectifiers," *IEEE Trans. Ind. Electron.*, Vol. 46, No. 4, pp. 788-795, Aug. 1999.
[28] Q. Zhao and F. C. Lee, "High-efficiency, high step-up DC-DC converters," *IEEE Trans. Power Electron.*, Vol. 18, No. 1, pp. 65-73, Jan. 2003.
[29] K. C. Tseng, J. T. Lin, and C. C. Huang, "High step-up converter with three-winding coupled inductor for fuel cell energy source applications," *IEEE Trans. Power Electron.*, Vol. 30, No. 2, pp. 574-581, Feb. 2015.
[30] Z. Chen, Q. Zhou, and J. Xu, "Coupled-inductor boost integrated flyback converter with high-voltage gain and ripple-free input current," *IET Power Electronics*, Vol. 8, No. 2, pp. 213-220, Feb. 2015.

Lung-Sheng Yang was born in Taiwan, ROC, in 1967. He received his Ph.D. degree in Electrical Engineering from the National Cheng-Kung University, Tainan, Taiwan, ROC, in 2007. He is presently working as an Associate Professor in the Department of Electrical Engineering, Far East University, Tainan, Taiwan, ROC. His current research interests include power factor correction, dc-dc converters, and renewable energy conversion.

Chia-Ching Lin was born in Taiwan, ROC, in 1959. He received his M.S. degree in Electrical Engineering from the National Cheng-Kung University, Tainan, Taiwan, ROC, in 2006. He is presently working as an Associate Professor in the Department of Electrical Engineering, Far East University, Tainan, Taiwan, ROC. His current research interests include power factor correction and dc-dc converters.

En-Chih Chang was born in Kaohsiung, Taiwan, in 1975. He received his B.S. degree from Feng-Chia University, Taichung, Taiwan, ROC, in 1999; his M.S. degree from the National Taiwan Ocean University, Keelung, Taiwan, ROC, in 2001; and his Ph.D. degree from the National Cheng Kung University, Tainan, Taiwan, ROC, in 2008, all in Electrical Engineering. He joined the Department of Electrical Engineering, I-Shou University, Kaohsiung, Taiwan, ROC, in 2009, as an Assistant Professor. His current research interests include sliding mode control, intelligent control, grey theory, and their applications in power electronics systems.